Partition of Manganese During the Proeutectoid Ferrite Transformation in Steel

J. B. GILMOUR, G. R. PURDY, AND J. S. KIRKALDY

The late stages of the isothermal proeutectoid ferrite reaction in Fe-C-Mn have been investigated theoretically and experimentally. For the growth of grain-boundary allotriomorphs three temporal regimes must be recognized. In the early regime the grain-size is infinite with respect to the diffusion length of carbon so the growth is parabolic. The middle regime involves the cumulative impingement of the carbon fields from opposite sides of the grains. This regime ends as the carbon activity approaches substantial uniformity through the ferrite and austenite. The final stage involves the extremely slow approach of the manganese towards uniform activity as well. These temporal regimes must be further subdivided into high and low supersaturation regions. In the low supersaturation region segregation of manganese must occur at all times, while in the high supersaturation region it must occur significantly only for late times. The growth rates and the diffusion profiles for the third temporal regime have been calculated on a local equilibrium model and compared with the metallographic and microprobe results for alloys within the two regions of supersaturation. The agreement between theory and experiment is in all cases good.

MOST substitutional alloying elements retard the rate of diffusion-controlled transformations in steel. The alloying effect on growth may be attributed to three factors:

1) The effect of the alloying element on the Fe-C phase diagram.
2) Ternary diffusion interactions.
3) Diffusion "drag" due to the slowly-diffusing alloying element.

Since manganese depresses the Ae_3 line we may expect that this addition will produce a strong retarding effect at a given temperature due to constitutional effects alone. Furthermore, since the proeutectoid reaction involves rejection of both carbon and manganese from the ferrite and since the ternary interaction between manganese and carbon is attractive, we may expect the positive manganese "spike" at the interface to retard the flow of carbon away from the interface and thus also retard the growth at certain stages of the transformation.[1]

According to the local equilibrium theory for growth into an infinite medium, there exist two regimes which are defined by the relative supersaturation. For high supersaturation, as indicated in Fig. 1,[2] the rate equations with $D_C >> D_{Mn}$ imply that there is no partition of manganese between the austenite and the ferrite so factor 3 is negligible in this regime. On the other hand, in the low supersaturation regime, partition must occur and diffusion control by the slowly-diffusing element takes over.

There is a distinct possibility that in both regimes for early times of transformation and in both the infinite and finite boundary conditions (the latter will always be effectively infinite for early enough times) the local equilibrium conditions may fail. One possible solution in such cases is the substitution of paraequilibrium[2,3] (or the approximately equivalent

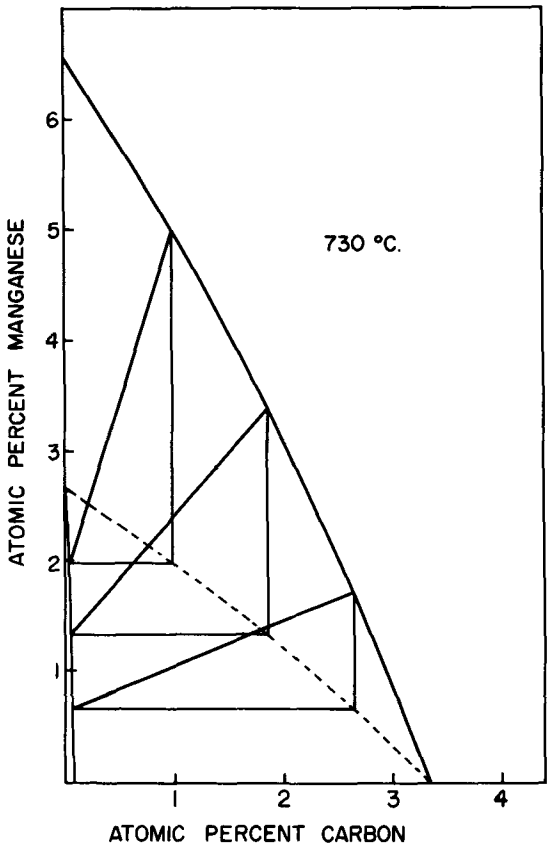

Fig. 1—730°C isotherm for iron-rich alloys in the Fe-C-Mn alloy systems.[2] The right triangles with tie-lines on the hypotenuse approximately define the boundary (----) between partition and no-partition reactions.[1]

J. B. GILMOUR is with the Corrosion Group, Physical Metallurgy, Mines Branch, Department of Energy, Mines, and Resources, Ottawa, Ontario, Canada. G. R. PURDY and J. S. KIRKALDY are Professor and Stelco Professor, respectively, Department of Metallurgy and Materials Science, McMaster University, Hamilton, Ontario, Canada.

Manuscript submitted April 17, 1972.

"no-partition" equilibrium[4]) for local equilibrium conditions. Unfortunately, a firm criterion for such a mode of transition has not yet been enunciated.

The present paper is concerned with a theoretical and experimental description of the late-time proeutectoid transformation in finite systems, *i.e.*, with grain boundary precipitation in multicrystalline austenite, so the aforementioned ambiguity of mode does not arise. However, the necessary conditions of carbon impingement from opposite sides of a grain lead to severe complications in the general solution of the diffusion equations, necessitating the introduction of approximate theoretical procedures.

In an earlier paper, the thermodynamics of the Fe-C-Mn system in the proeutectoid ferrite region were elucidated via theory and confirmatory experiments.[2] Fig. 1 shows the constitutional results for one temperature of interest. These new data were used by Gilmour[5] to analyze the early kinetic observations of Purdy *et al.*[1] and Kinsman and Aaronson.[6] The same thermodynamic data are used as the basis for the kinetic predictions presented herein. It is demonstrated that these data along with published diffusion data, combined with an approximate local equilibrium model, correctly predict the kinetics for both high and low supersaturation conditions. The related problem of growth of carbides in stainless steel has been discussed in detail by Strawstrom and Hillert.[7]

Of particular note are the experimental methods used here for measuring and interpreting interface diffusion profiles which have half-widths as small as 0.5 μ.

THEORY

The following calculations deal with the one-dimensional growth of planar grain boundary allotriomorphs from opposite sides of a grain as indicated schematically in Fig. 2. This process may be considered in three stages. The first involves parabolic growth from both sides according to the earlier exact calculations.[5] The time for this stage will depend on the time for the beginning of substantial carbon impingement from opposite sides of the boundary. During the second stage of impingement the driving force due to the carbon activity gradient is gradually reduced and the transformation rate correspondingly decreases to a value consistent with a uniform and equal carbon chemical potential in both phases. This stage is followed by the slow partition of manganese from the ferrite to the austenite controlled by manganese diffusion. In the analysis we must distinguish between parabolic primary stages at high and low supersaturation, which are in turn distinguished by no-partition and partition of manganese, respectively.

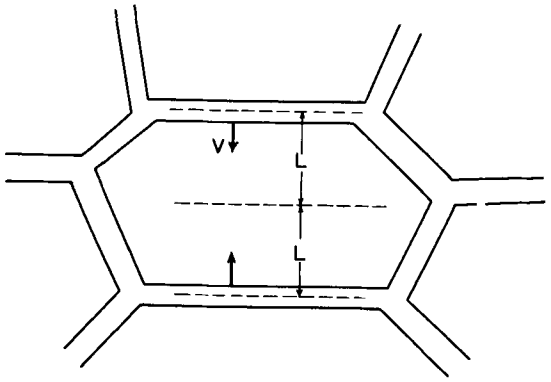

Fig. 2—Model for "one-dimensional" growth of grain boundary allotriomorphs.

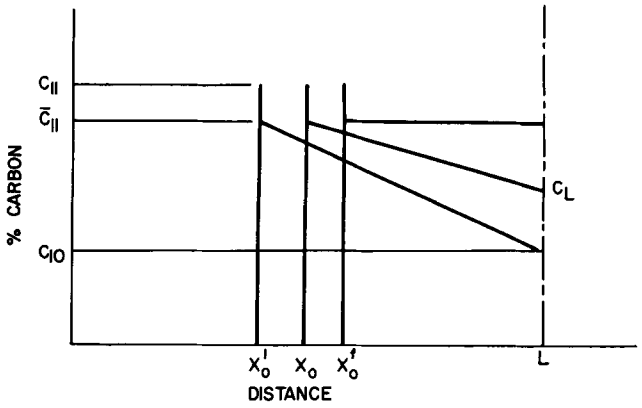

Fig. 3—Carbon concentration profile for the calculation of impingement time.

High Supersaturation Case

While an exact solution is available for the early stages of transformation there are no analytical solutions to the diffusion equations for the variable boundary conditions involved in stages 2 and 3 so approximate and (or) iterative procedures must be used. Iterative solutions for this type of problem using computer techniques have been published.[8] However, we have developed solutions patterned after Zener's[9] approximation (with the error function represented as a triangle as in Fig. 3) which are sufficiently accurate for our pruposes. Of course, the carbon diffusion fields begin to impinge very early, for an error function has a finite value for all but infinite arguments, but the effect of the extended tail of the distribution on the growth rate will be negligible until the centerline accumulation has reached about 20 pct. Thus for the purposes of this approximate calculation we have found it satisfactory to assume that the interface (for a planar grain) will move parabolically to a position (X_o')* as defined in Fig. 3 such that the triangular representation of the error function defines the initiation of impingement, and the mass within this triangle equals the mass removed from the α phase, viz.,

$$\frac{1}{2}(\bar{C}_{11} - C_{10})(L - X_0') = C_{10}X_0' \quad [1]$$

or

$$X_0' = \frac{L(\bar{C}_{11} - C_{10})}{(\bar{C}_{11} - C_{10})} \quad [2]$$

where

$$\bar{C}_{11} = C_{11} + \frac{D_{12}}{D_{11}}(C_{21} - C_{20}) \quad [3]$$

is the effective carbon concentration driving the trans-

*The concentration notation used is that of Purdy *et al.*[5] and summarized here Primed quantities refer to the ferrite and unprimed quantities refer to the austenite. The first subscript refers to the alloying element, carbon 1, or manganese 2 and the second subscript refers to the location: the interface 1, or the bulk 0. Thus C_{21} refers to the Manganese concentration in austenite at the interface. All other quantities are defined in Fig. 3.

formation. This latter relation corrects the local equilibrium value C_{11} for the ternary interaction of the carbon profile with the associated steep manganese profile (not shown). It is equal to the ratio of the off-diagonal to on-diagonal diffusion coefficients and can be expressed thermodynamically by

$$\frac{D_{12}}{D_{11}} = \epsilon_{12} N_1 \qquad [4]$$

where ϵ_{12} is the Wagner interaction parameter and N_1 is the average mole fraction of carbon in the interaction zones.[10] The position of the interface when the carbon first reaches uniform activity is again given by the appropriate mass balance and is equal to

$$X_0^f = L\left(1 - \frac{C_{10}}{\bar{C}_{11}}\right) \qquad [5]$$

In both calculations the mass of carbon in the spike at the interface due to the thermodynamic interaction with manganese has been neglected.

When $X_0' < X_0 < X_0^f$ we may show from the carbon mass balance that

$$C_L = \frac{2LC_{10} - \bar{C}_{11}(L - X_0)}{L - X_0} \qquad [6]$$

where C_L is the concentration of carbon at the center of the grain. When the carbon reaches uniform activity, $C_L = \bar{C}_{11}$. Finally when Eq. [6] is combined with the instantaneous interfacial carbon mass balance

$$\bar{C}_{11} \frac{dX_0}{dt} = -D \frac{dC}{dx} \qquad [7]$$

we obtain the differential equation

$$\frac{dX_0}{dt} = \frac{2D_{11}(X_0^f - X_0)}{(L - X_0)^2} \qquad [8]$$

This velocity expression may then be integrated to yield the time vs interface position

$$t_i = \frac{1}{2D_{11}}\left\{\frac{1}{2}[X_0'^2 - X_0^2] + [2K + X_0^f][X_0 - X_0'] - K^2 \ln\left[\frac{X_0^f - X_0}{X_0^f - X_0'}\right]\right\} \qquad [9]$$

where

$$K = L\frac{C_{10}}{\bar{C}_{11}} \qquad [10]$$

The total time of transformation is therefore the time required for the interface to move parabolically to X_0 plus the impingement time defined by relation [9]. A similar but simpler Zener type calculation for the time to the beginning of impingement yields

$$t_b = \frac{C_{10}\bar{C}_{11}}{(\bar{C}_{11} + C_{10})^2} \cdot \frac{L^2}{D} \qquad [11]$$

Fig. 4 shows the evaluations of t_i, t_b, and $t_i + t_b$ for various grain half-widths in a 1.5 at. pct Mn, 0.45 at. pct C alloy transformed at 728°C. Here we have used the carbon diffusion data estimated by Kaufman *et al.*[11] and assumed complete impingement at $X_0 = 0.99\, X_0^f$. It is evident that even for the largest grain sizes usually encountered in alloy steels, the carbon will reach uniform activity in a few hours. As the diffusion coefficient for manganese in this temperature range is of

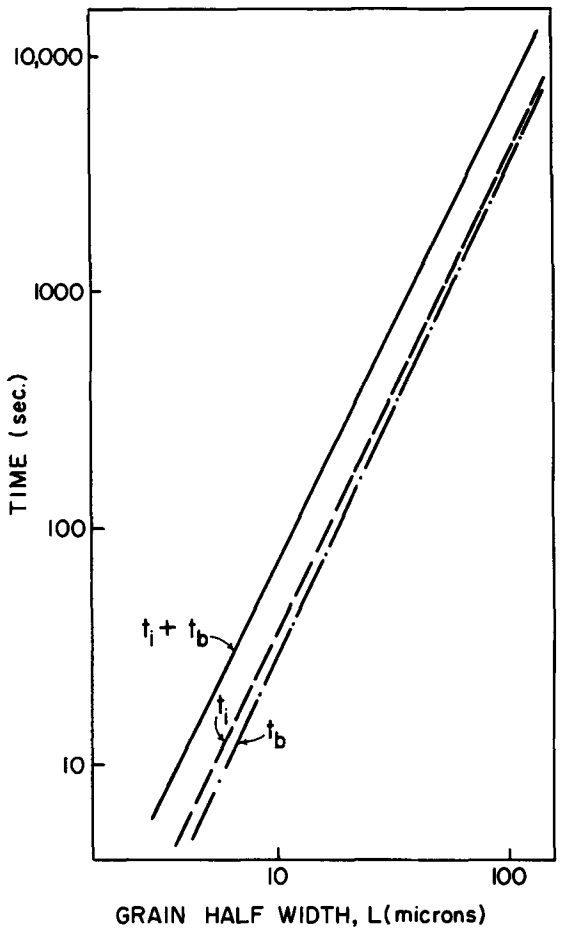

Fig. 4—Time ($t_i + t_b$) required for the interface to reach $0.99\, X_0^f$. Calculated for a 0.45 at. pct C, 1.5 at. pct Mn alloy at 728°C.

the order 10^{-14} cm^2/s,[12] the amount of partition of this element during the initial impingement period will be negligible.

Since the time of impingement t_i is relatively short, the interfacial manganese concentrations cannot have changed appreciably from those predicted by the solution to the diffusion equations for times up to t_b. The conditions for subsequent redistribution of manganese can therefore be represented as in Fig. 5. The diffusion coefficient for manganese in ferrite is about two orders of magnitude higher than in austenite[5] so we may assume that the manganese gradient in the ferrite is negligible and its content C_{21}' is uniformly lowered, Fig. 5. In addition, the mass of carbon in the carbon spike can again be ignored because

$$(C_{11} - \bar{C}_{11})\frac{a}{2} << (\bar{C}_{11} - C_{10})(L - X_0) \qquad [12]$$

As the manganese diffuses out of the ferrite and the interface moves slowly forward, the tie-line representing the interface must move towards the equilibrium position. Since it has been assumed that the interface is in local equilibrium, the specification of any one interface concentration automatically fixes all other concentrations. A convenient choice for the independent concentration is C_{21}'. The analysis again follows a Zener type approximation with control by manganese diffusion, the tie-line moving such that the rapidly adjusting carbon distribution remains very close to the conditions of uniform activity.

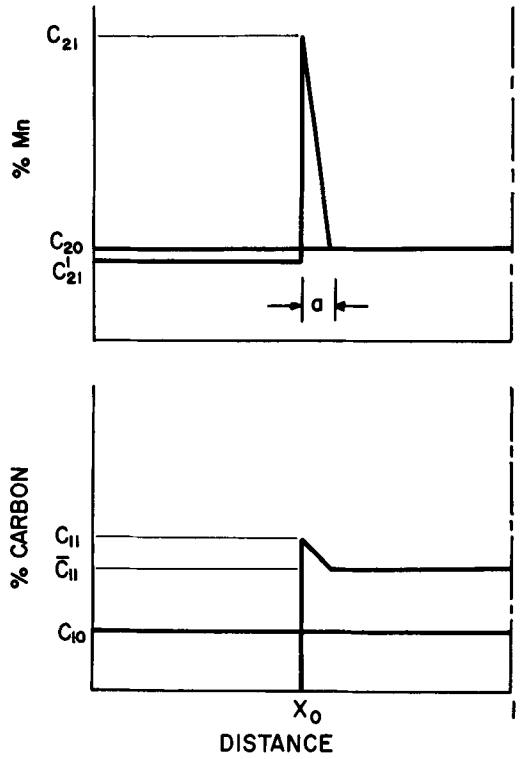

Fig. 5—Approximate concentration profiles for manganese diffusion control at long times in highly supersaturated alloys.

Now referring again to Fig. 5, the carbon mass balance (ignoring the area under the carbon spike) gives

$$X_0 = \left[\frac{\bar{C}_{11} - C_{10}}{\bar{C}_{11}}\right] L \qquad [13]$$

where L is again the half-width of a planar grain and X_0 the position of the interface. Letting

$$F_1(C'_{21}) = \frac{\bar{C}_{11} - C_{10}}{\bar{C}_{11}} \qquad [14]$$

then

$$X_0 = F_1(C'_{21})L \qquad [15]$$

and

$$\frac{dX_0}{dt} = L\,\frac{dF_1(C'_{21})}{dt} \qquad [16]$$

From the bulk manganese mass balance we have as well that

$$a = 2X_0\left[\frac{C_{20} - C'_{21}}{C_{21} - C_{20}}\right] \qquad [17]$$

The instantaneous mass balance for manganese may then be written

$$\frac{D_{22}}{a}(C_{21} - C_{20}) = (C_{21} - C'_{21})\,\frac{dX_0}{dt} \qquad [18]$$

where D_{22} is the diffusion coefficient for manganese in austenite.

Eqs. [15], [17], and [16] may be substituted into Eq. [18] to yield

$$\frac{D_{22}}{2L^2}\,\frac{[C_{21} - C_{20}]^2}{[C_{20} - C'_{21}][C_{21} - C'_{21}]} = F_1(C'_{21})\,\frac{dF_1(C'_{21})}{dt} \qquad [19]$$

Letting

$$\frac{[C_{21} - C_{20}]^2}{[C_{20} - C'_{21}][C_{21} - C'_{21}]} = F_2(C'_{21}) \qquad [20]$$

then

$$\frac{D_{22}}{2L^2}\,dt = \frac{F_1(C'_{21})}{F_2(C'_{21})}\,dF_1(C'_{21}) \qquad [21]$$

and

$$\phi = \frac{D_{22}}{2L^2}\,t = \int_{F_1(C'_{21} = C_{20})}^{F_1(C'_{21})} \frac{1}{2}\,\frac{d\{F_1(C'_{21})\}^2}{F_2(C'_{21})} \qquad [22]$$

If the tie-lines on the ternary isotherm are known empirically then this expression can be graphically or numerically integrated from $C'_{21} = C_{20}$ (the unpartitioned manganese content of the ferrite) to any lower value. This expression accordingly predicts the time dependence of the partitioning of the manganese, a quantity which can be compared with experiment.

Low Supersaturation

The solution to the diffusion equations for alloys transformed in the regime of low supersaturation[5] under the local equilibrium assumption predicts manganese partitioning for all times and therefore that the transformation rate will always be extremely small. This means that for all times which are reasonably accessible experimentally (<1 year, say) the carbon profile, whether in the nonimpingement or impingement time range, will have a negligible effect on the kinetics and the pseudobinary solution for growth by manganese control is applicable. The alloy carbon content serves only to help determine the interface tie-line. This solution is[5]

$$C_2 = C_{20} + \frac{(C_{21} - C_{20})\ erfc\ \lambda/2\sqrt{D_{22}}}{erfc\ \beta} \qquad [23]$$

where

$$\lambda = x/\sqrt{t} \qquad [24]$$

$$\beta = \alpha/2\sqrt{D_{22}} \qquad [25]$$

and α is the position of the interface in λ-space. β can be obtained as a solution of the transcendental equation

$$\beta = \frac{1}{\sqrt{\pi}}\,\frac{(C_{21} - C_{20})}{(C_{21} - C'_{21})}\,\frac{e^{-\beta^2}}{erfc\ \beta} \qquad [26]$$

The particular tie-line applicable is that corresponding to a carbon content of

$$C_{11} = C_{10} - \frac{D_{12}}{D_{11}}[C_{21}(C_{10}) - C_{20}] \qquad [27]$$

EXPERIMENTAL

Materials and Methods[4]

Since preliminary experiments showed that localized manganese increases at the interface between the growing ferrite and the original austenite could be readily detected in highly supersaturated alloys only after times exceeding a day, a series of long-time experiments were carried out in Alloy A, 0.45 at. pct C, 1.5 at. pct Mn, prepared as described elsewhere.[2] The samples were encapsulated in small evacuated silica

tubes back-filled with one-third atmosphere of argon. They were austenitized for 19 h at 1200°C and then rapidly transferred to a furnace preheated to 728°C. This rapid transfer was accomplished by placing two Kanthal tube furnaces end to end and sliding the capsule from one hot zone to the other. At the end of the transformation time (two days to two months) the capsules were rapidly withdrawn from the furnace and the samples quenched by breaking the vacuoles under water. From the time the capsule left the hot zone until it was broken under water was less than three seconds. During the isothermal transformation the furnace temperature was periodically monitored with a standardized Pt-Pt 10 pct Rh thermocouple and was controlled to ±1°C of the desired temperature.

Another series of experiments using the same technique were carried out on Alloy B, 1.11 at. pct C, 2.09 at. pct Mn alloy at 728°C. At this temperature this alloy lies just outside of the zone of zero partition[5] as predicted by the local equilibrium analysis and therefore should show manganese partition for all times.

The manganese partition was investigated experimentally using the modified electron microprobe analytical technique described below.

A Convolution Technique for Interpreting the Microprobe Results for Steep Concentration Profiles[4]

The spatial X-ray intensity distribution from a specimen with steep concentration profiles is the convolution of the true profile with what is known as the "probe function". This function is the spatial intensity distribution of the emitted characteristic X-ray line being investigated, normalized so as to be concentration independent. The spread of the function is determined by the beam width and the scattering of the electrons in the target material. If this function can be determined empirically under conditions which correspond closely to those in the analysis then it is possible to mathematically deconvolute the experimentally determined profile to yield the true concentration curve. In the present study we have found it more profitable to perform the "forward" calculation. The empirical probe function is convoluted with a theoretical concentration profile and the calculated curve compared with experiment. Convolutions of this type may be readily carried out using numerical methods and machine computation.

In this experiment the probe function was experimentally determined by passing the beam over a known concentration step obtained by clamping together two alloys (similar to the material to be analyzed), sectioning at right angles to the interface and polishing. Fig. 6 shows the result of a step scan across the Fe-Fe 3.5 pct Mn couple. A simple automatic timing device activated the sample to move in accurately reproducible steps of $\frac{1}{3}$ μ.

If the probe function is gaussian, then the empirical probe trace will be an error function. Inversely, if the probe trace is an error function as in our experiment, then the conjugate probe function is determined by the parameter "d" in Fig. 6. The normalized gaussian is then

$$g(x) = \frac{1}{d} \exp - \frac{\pi}{4}\left[\frac{x}{d}\right]^2 \qquad [28]$$

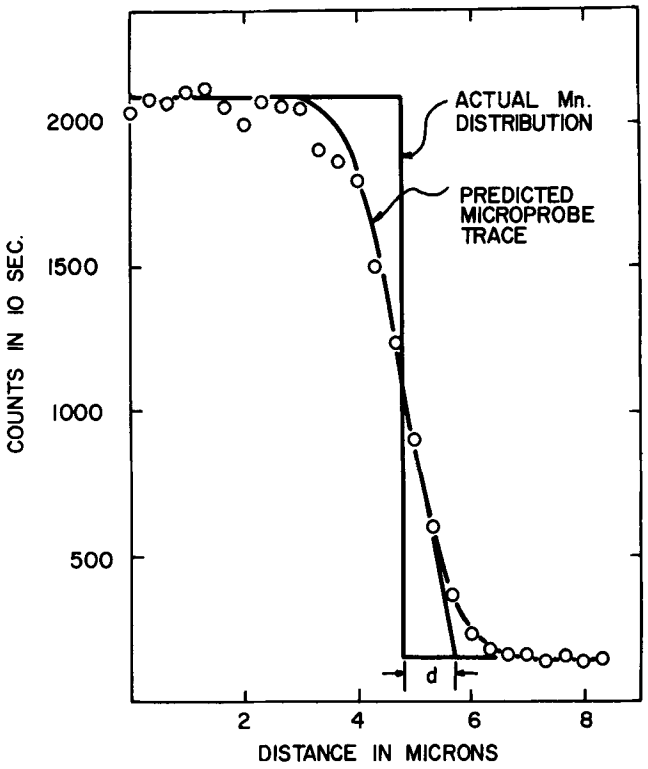

Fig. 6—Electron probe microanalysis of a manganese concentration step. Predicted line is assuming a gaussian probe function with $d = 0.9$ μ.

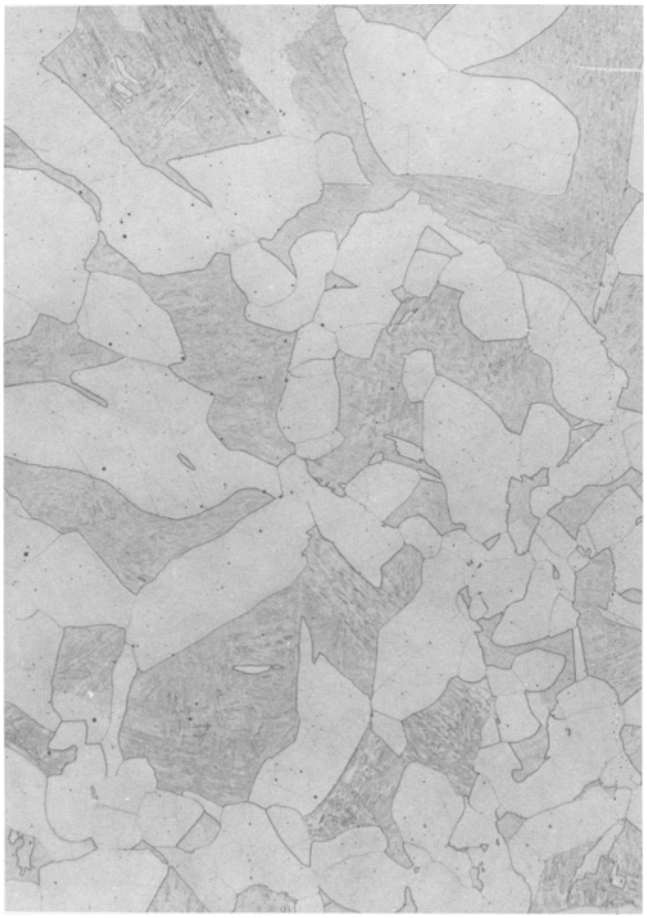

Fig. 7—Micrograph typical of samples of alloy A (0.45 at. pct C, 1.50 at. pct Mn) transformed at 728°C for 2 d to 2 month. Magnification 75 times.

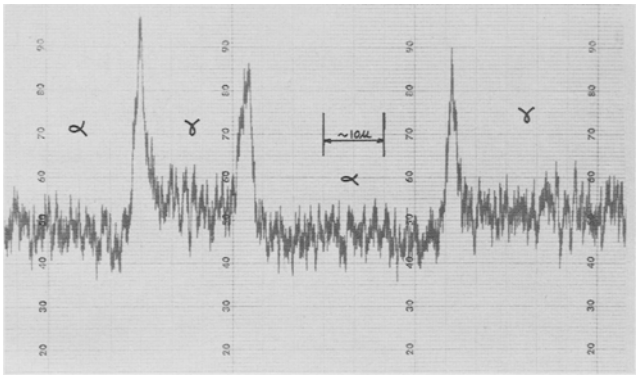

Fig. 8—A typical microprobe scan across a sample of alloy A transformed for 5.37×10^6 s (2 month) at 728°C.

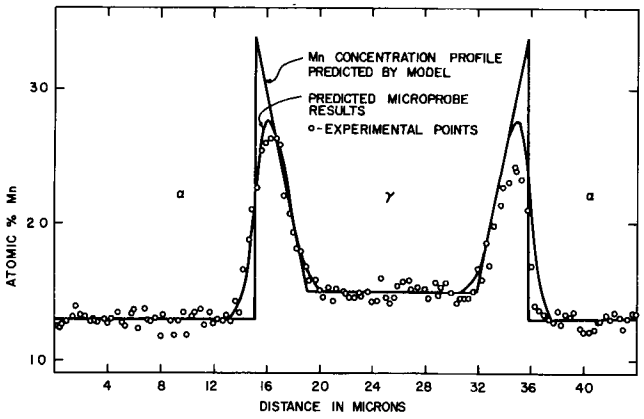

Fig. 9—Detailed microprobe analysis of alloy A transformed for 5.37×10^6 s (2 month) at 728°C.

and is in the precise form required for a forward convolution calculation.

RESULTS AND DISCUSSION

High Supersaturation

Fig. 7 is a micrograph typical of all samples of Alloy A transformed at 728°C for periods varying from 2 d to 2 month. These samples consist of a relatively blocky ferrite-martensite (former austenite) mixture. Fig. 8 is a preliminary microprobe trace across an area of the sample transformed for about 2 months. This trace is similar to that obtained for all samples, except that the size of the peaks due to the local increase of manganese at the phase boundary is generally less in samples transformed for shorter times.

Figs. 9 to 13 contain the results of the electron probe microanalysis of these specimens. In all cases the austenite distant from the interface was used as a probe standard, the background being measured on a sample of Ferrovac E.

The experimental points on Figs. 9 to 13 were determined by detecting the manganese K_α radiation and point counting for 10 s, using the step-scan procedure mentioned above. The raw counts were corrected for background and the manganese concentration was calculated assuming linearity of the concentration vs X-ray intensity relationship.[4]

All specimens, with the exception of the one transformed for 2 d, showed a noticeable increase of manganese at all ferrite-austenite interfaces. In many cases the observed peak height was not as great as those presented in the figures, but in these cases the increase was spread over a greater distance. These results undoubtedly correspond to grain boundaries

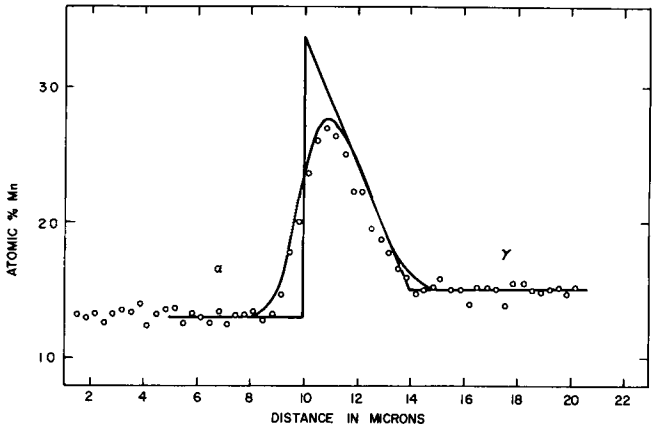

Fig. 10—Microprobe analysis of alloy A transformed for 5.37×10^6 s (2 month) at 728°C.

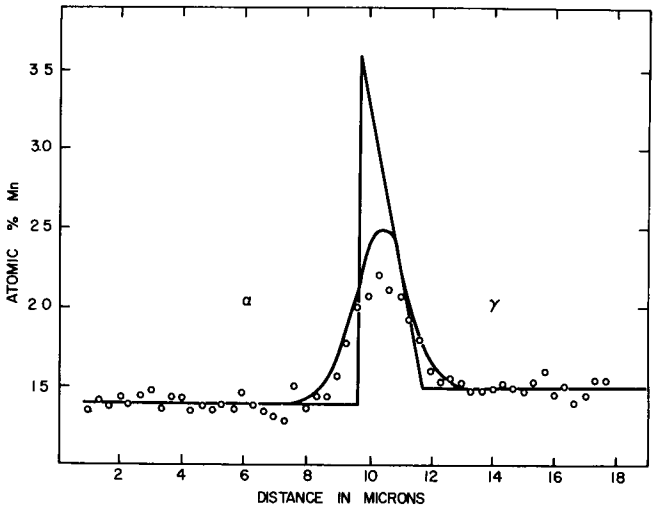

Fig. 11—Microprobe analysis of alloy A transformed for 1.78×10^6 s (20 d) at 728°C.

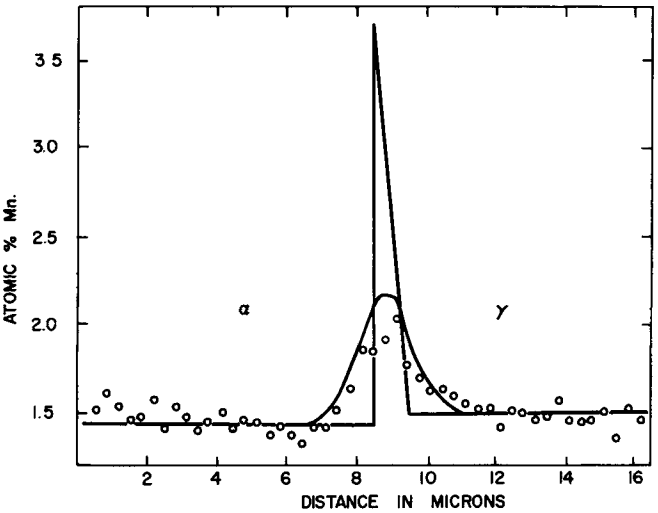

Fig. 12—Microprobe analysis of alloy A transformed for 5.12×10^5 s (6 d) at 728°C.

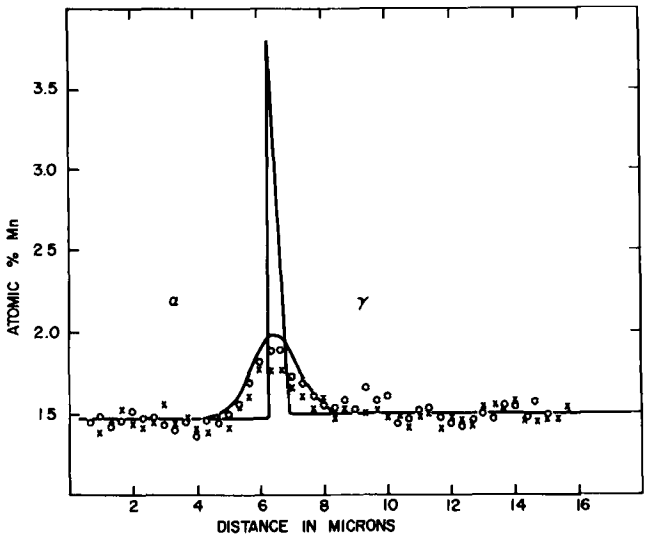

Fig. 13—Microprobe analysis of alloy A transformed for 1.6 × 10^5 s (2 d) at 728°C.

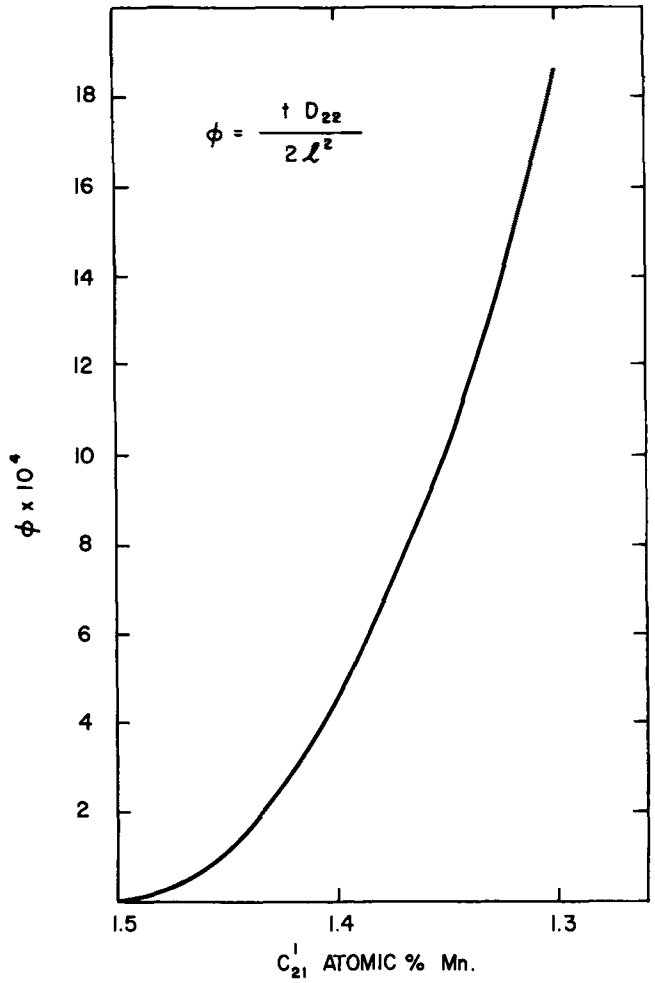

Fig. 14—The calculated relationship between C'_{21} and ϕ for a 0.45 at. pct C, 1.5 at. pct Mn alloy at 728°C.

which intersect the surface at an oblique angle. The observed increase in manganese at ferrite-austenite interfaces in the 2 d sample was so small that at many interfaces it was screened by the random scatter of the point counts. Nonetheless, Fig. 13 shows the

Table I. Data Required for Calculation of Manganese Concentration Curves

Figure	9	10	11	12	13
Time, s	5.37×10^6	5.37×10^6	1.78×10^6	5.12×10^5	1.6×10^5
C'_{21}	1.30	1.30	1.44	1.44	1.47
C_{21}	3.38	3.38	3.72	3.72	3.80
F_1, C'_{21}	0.7472	0.7472	0.7129	0.7129	0.7044
ϕ	1.863×10^{-3}	1.863×10^{-3}	1.62×10^{-4}	1.62×10^{-4}	4.03×10^{-5}
L, μ (calc)	24.6	24.6	48	25.7	30
L, μ(est*)	35	45	60	70	50
a	3.9	3.9	1.9	1.0	0.6
d, μ	1	1	0.9	0.9	0.9

*Estimated from microstructure.

positive results of two step scans across the same interface in this particular sample.

The integral ϕ from Eq. [22] was evaluated for a variation in C'_{21} from the initial value $C'_{21} = C_{20} = 1.50$ at. pct Mn to 1.30 at. pct Mn at intervals of $\Delta C'_{21}$ 0.01 at. pct Mn. The limiting tie-lines for $C'_{21} = 1.5$ at. pct and $C'_{21} = 1.3$ at. pct Mn were evaluated by the methods described in Ref. 1 and it was assumed that the distribution coefficient for manganese varied linearly in this range between the limiting values of 0.3876 and 0.3846, Fig. 1. From this we obtain

$$C_{21} = \frac{C'_{21}}{0.3651 + 1.5\,C'_{21}} \qquad [29]$$

The value of C_{11} was calculated from C_{21} assuming that the $\alpha + \gamma/\gamma$ phase boundary was linear, thus generating

$$C_{11} = -0.592\,C_{21} + 0.0391 \qquad [30]$$

$\bar{C}_{11}$ was calculated using Eq. [3], the value D_{12}/D_{11} from expression [4] and the ternary diffusion data given by Brown and Kirkaldy,[13] evaluated at C_{11}. Thus all of the concentrations necessary for the evaluation of $F_1(C'_{21})$ and $F_2(C'_{21})$ are known so the integral can be numerically evaluated. Fig. 14 shows the result of this integration, ϕ being plotted as a function of C'_{21}.

The experimental results were compared with the model in two ways using the data in Table I. Firstly, from the penetration curves the average difference in manganese concentration between the ferrite and the austenite distant from the interface $(C_{20} - C'_{21})$ was recorded. This difference fixes the value of ϕ, and thus using the extrapolated data of Wells and Mehl[12] for D_{22}, the time of the experiment for t, a value of L is obtained from Eq. [22], *viz.*,

$$L = \sqrt{D_{22}\,t/2\phi} \qquad [31]$$

Ideally, we should have been given L as an initial parameter and from this calculated $C_{20} - C'_{21}$ for comparison with experiment. In view, however, of the general unreliability of the observed L's, as described below, we have chosen to proceed in this way.

In the model, L represents the half-width of an idealized elongated grain, as indicated in Fig. 2. An estimate of this distance was made from direct observation of the sample while a particular elongated grain was being analyzed in the microprobe. These estimated values are compared with those calculated in Table I and the agreement is seen to be satisfactory, in view of the uncertainties in the observed values of L and $C_{20} - C'_{21}$. We believe that the systematic short-

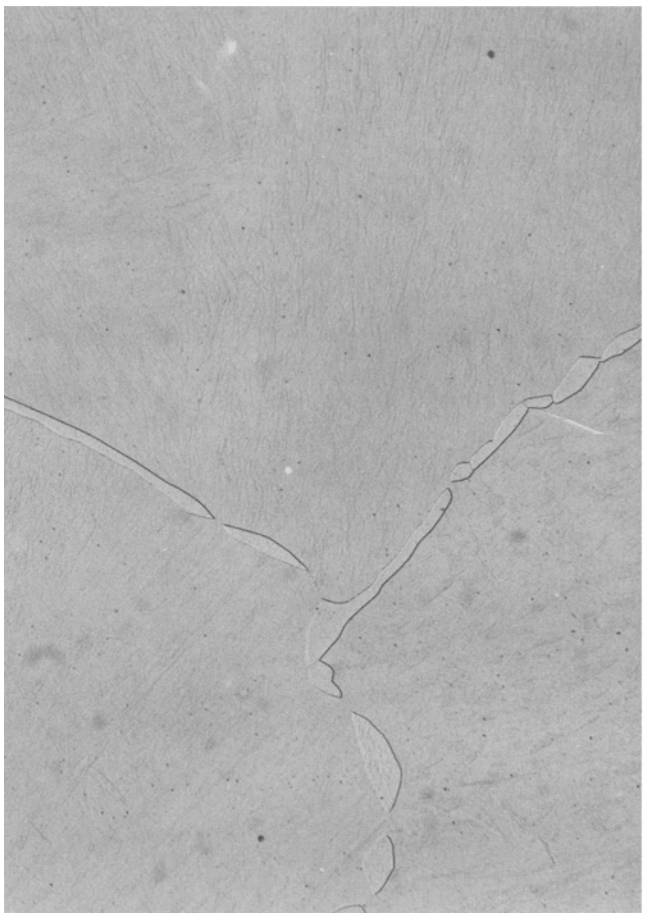

Fig. 15—Typical micrograph of alloy B (2.09 at. pct Mn, 1.11 at. pct C) transformed for 4.32×10^5 s (5 d) at 728°C. Magnification 295 times.

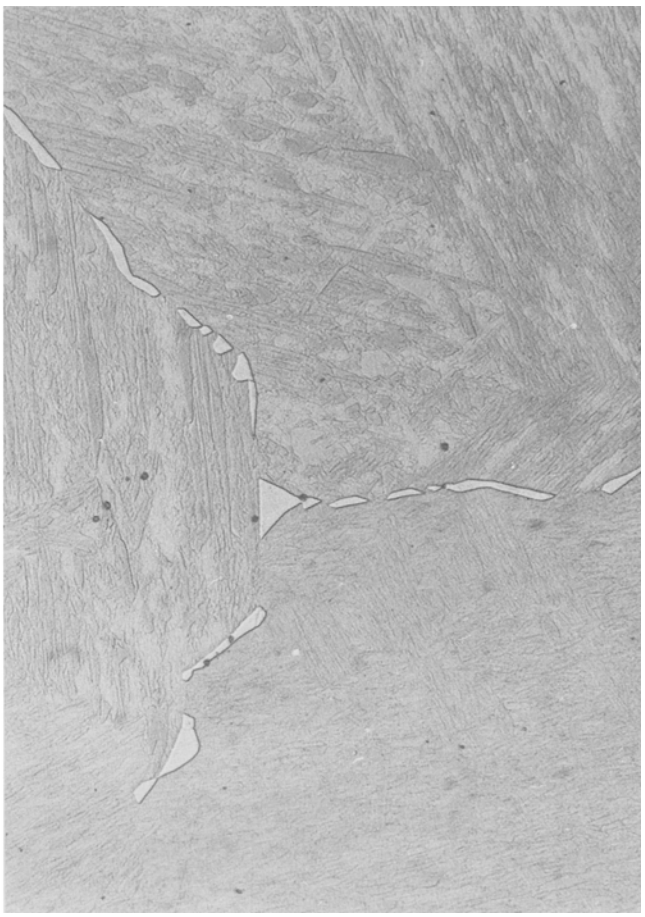

Fig. 16—Typical micrograph of alloy B transformed for 3.15×10^6 s (37 d) at 728°C. Magnification 295 times.

fall in these calculated values of L are due to the inadequacy of the planar model of Fig. 1 as a representation of the more frequently occurring equi-axed configuration.

A more precise closure between theory and experiment can be found in the experiment described by Fig. 9. Since, in this case, the center-line of the grain is uniquely located at the 25.5 μ position and the mass balance locates the origin of growth at about -2 μ, $L = 27.5$ μ, which is in excellent agreement with the calculated value of 24.6 μ. This is in turn theoretically consistent with the observed $C_{20} - C'_{21}$.

As a second test, we have used the basic data to predict the observed concentration profiles. The width of the base of the manganese spike, a, was calculated from Eq. [17] and its height is given by Eq. [29]. This predicted profile was then convoluted at 0.2 μ intervals with the gaussian microprobe distribution function corresponding to Fig. 6. Since the precise interface location is not initially known the curves shown in Figs. 9 to 13 have been positioned laterally with respect to the experimental curves via a visual best fit. It may be seen that the agreement between the predicted or theoretical microprobe curves and the experimental results is in general excellent.

In the development of the model for these late times it was assumed that the manganese gradients in the ferrite are negligible. Figs. 9 to 11 indicate that this is a good assumption for experiments of long duration (20 d and 2 month). However, Fig. 12 (6 d) suggests that a nonzero gradient of manganese may exist in the ferrite near the interface for shorter times.

The model used in the calculation does not require that the interface concentrations throughout a sample be uniform. Various interface concentrations may coexist in the sample, changing according to the effective value of L in Eq. [22]. From the observations it appears, as expected, that these variations will be greater early in the transformation. The rather uniform ferrite composition from grain to grain observed in the 2 month sample is undoubtedly due to the redistribution of carbon to uniform activity over the whole sample, thus forcing the ferrite-austenite interfaces towards a common tie-line in the ternary phase diagram.

Low Supersaturation

To test the local equilibrium model for the regime of low supersaturation, several transformation experiments were carried out with alloy B (1.11 at. pct C, 2.09 at. pct Mn) at 728°C. According to the phase diagram this alloy lies just outside the area of zero partition and the solution to the diffusion equations[5] requires the redistribution of manganese for all times of transformation.

Figs. 15 and 16 show grain boundary precipitates

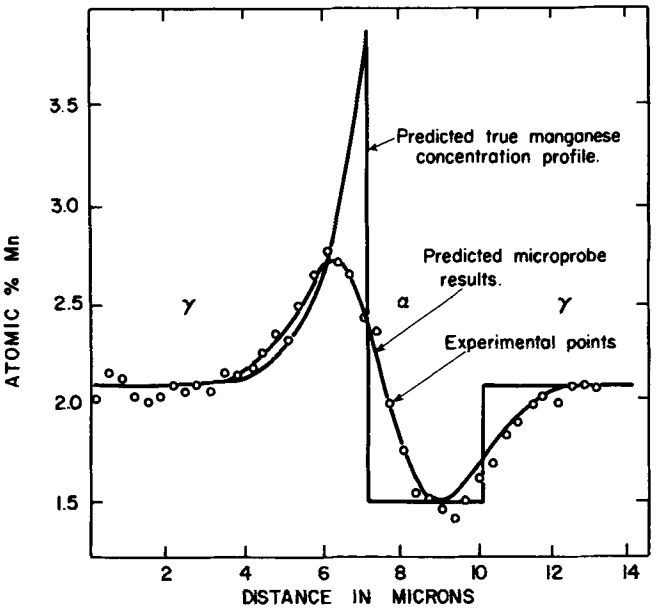

Fig. 17—Microprobe analysis of alloy B transformed for 5 d at 728°C.

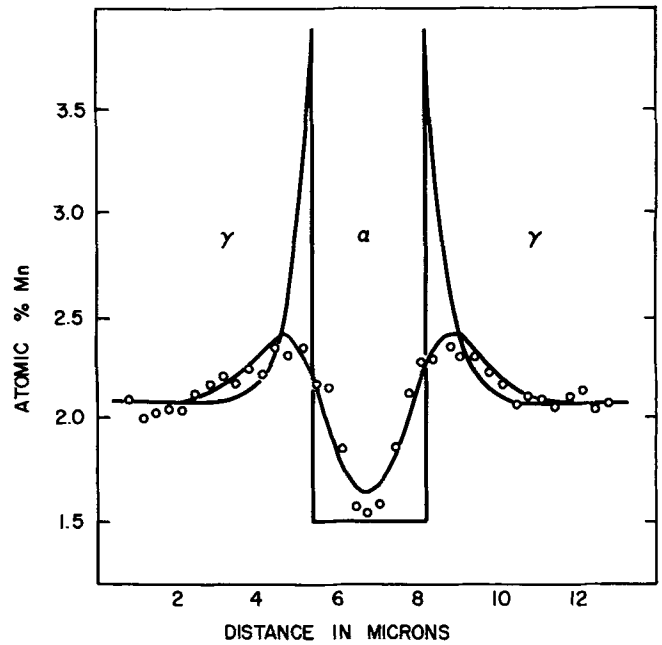

Fig. 18—Microprobe analysis of alloy B transformed for 3 × 10^6 s (37 d) at 728°C.

formed after annealing for 5 and 37 d, respectively. It is noted that the precipitating ferrite does not form a continuous layer at the austenite grain boundaries. In many areas the ferrite develops as a line of small equiaxed precipitates and these grow together at later times to form a relatively continuous layer of ferrite at the grain boundary.

Attempts to determine the growth rate of the ferrite in these samples were unsuccessful due to the unsatisfactory morphological history of the precipitates and the uncertainty of nucleation times. Many of the equiaxed precipitates are rejecting manganese in many directions and thus grow faster than predicted by the model for the uniform growth of planar grain boundary precipitates.

Fig. 17 shows a microprobe trace for a relatively thick precipitate in the sample transformed for 5 d. The local equilibrium model leading to Eqs. [23] and [26] specifies that $C_{21} = 3.9$ at. pct Mn and $C'_{21} = 1.5$ at. pct Mn and results in a growth rate parameter $\beta = 0.97$. This precipitate was 3 μ thick corresponding to a diffusion coefficient for manganese of 5×10^{-14} cm^2/s. By comparison, the data of Wells and Mehl[12] extrapolated to this temperature suggest a value of 4×10^{-15} cm^2/s. Nevertheless, the convoluted curve calculated using the solutions to the diffusion equations, Eqs. [23] and [26], and the Wells-Mehl value of D_{22} agrees very well with the experimentally observed result. Appreciable deviations of the angle of intersection of this precipitate with the surface could account for its width, but if this were in fact the case, the buildup of manganese ahead of the interface would appear less, so the inconsistency would remain. We must, therefore, assess the closure between theory and observation for this experiment as only fair.

On the basis of a large number of microprobe results such as Fig. 17, we conclude that most of the precipitates in this 5 d sample are growing only into one austenite grain, presumably the inactive interface is partially coherent as a remnant of the nucleation step, as predicted by C. S. Smith.[14]

In the sample transformed for 37 d, on the other hand, many of the precipitates analyzed showed a buildup of manganese at both interfaces in contact with the austenite as shown in Fig. 18. To fit this particular curve a value of $D_{22} = 1.7 \times 10^{-15}$ cm^2/s has been used, which is in good agreement with the Wells and Mehl value. The interface concentrations are empirically the same as given above for the 5 d sample, as required by the theory.

CONCLUSION

Approximate solutions to the diffusion equations assuming a local equilibrium interface have been developed for the very late stages of the proeutectoid ferrite transformation in highly supersaturated Fe-C-Mn alloys. The manganese concentration profiles near the ferrite-austenite interface, as detected with the electron probe microanalyzer, are in good agreement with the predictions based on the local equilibrium model.

Similarly, electron probe microanalysis of the manganese distributions in Fe-C-Mn alloys transformed in the pro-eutectoid zone of low supersaturation show fair to good agreement with the predictions of the parabolic local equilibrium model for times greater than 1 d.

In both zones, the manganese profiles are too narrow to be detected by our own optimal microprobe procedures for reaction times of less than 1 d.

ACKNOWLEDGMENTS

This work was made possible by a grant to J. S. Kirkaldy from the American Iron and Steel Institute. J. B. Gilmour is pleased to acknowledge the award of a Stelco Graduate Research Fellowship. G. R. Purdy is grateful for the award of a C. D. Howe Memorial Fellowship. The critical comments of our colleague, R. Sharma, were very valuable.

REFERENCES

1. G. R. Purdy, D. H. Weichert, and J. S. Kirkaldy: *Trans. TMS-AIME,* 1964, vol. 230, p. 1025.
2. J. B, Gilmour, G. R. Purdy, and J. S. Kirkaldy: *Met. Trans.,* 1972, vol. 3, p. 1455.
3. M. Hillert: *Inst. of Metals, Monograph No.* 33, 1961, p. 231.
4. H. I. Aaronson, H. A. Domian, and G. M. Pound: *Trans. TMS-AIME,* 1966, vol. 236, p. 768.
5. J. B. Gilmour: Ph.D. Thesis, McMaster University, Hamilton, Ontario, September, 1970.
6. K. R. Kinsman and H. I. Aaronson: *Transformation and Hardenability in Steels,* Climax Molybdenum, Ann Arbor, 1967.
7. C. Strawstrom and M. Hillert: *J. Iron Steel Inst.,* 1969, vol. 207, p. 77.
8. R. A. Tanzilli and R. W. Heckel: *Trans. TMS-AIME,* 1968, vol. 242, p. 2313.
9. C. Zener: *J. Appl. Phys.,* 1949, vol. 20, p. 950.
10. J. S. Kirkaldy and G. R. Purdy· *Can. J. Phys.,* 1962, vol. 40, p. 208.
11. L. Kaufman, S. V. Radcliffe, and M. Cohen: *Decomposition of Austenite by Diffusional Processes,* V. F. Zackay and H. I. Aaronson, eds., p. 342, Interscience, 1962.
12. C. Wells and R. F. Mehl: *AIME Trans.,* 1941, vol. 145, p. 315.
13. L. C. Brown and J. S. Kirkaldy: *Trans. TMS-AIME,* 1964, vol. 236, p. 223.
14. C. S. Smith: *Trans. ASM,* 1953, vol. 45, p 533.